

Infrared and millimeter observations of the galactic superluminal source GRS 1915 + 105

S. Chaty¹, I.F. Mirabel¹, P.A. Duc¹, J.E. Wink², and L.F. Rodríguez³

¹ Service d'Astrophysique, CEA/DSM/DAPNIA/SAP, Centre d'études de Saclay, F-91191 Gif-sur-Yvette Cedex, France

² IRAM, 300, rue de la Piscine, Domaine Universitaire de Grenoble, F-38406 Saint-Martin-d'Hères Cedex, France

³ Instituto de Astronomía, UNAM, Apdo Postal 70-264, México, DF, 04510, Mexico

Received 16 August 1995; accepted 13 November 1995

Abstract. Millimeter observations of the galactic source of relativistic ejections GRS 1915 + 105 (Mirabel & Rodríguez 1994) are consistent with this source being at a kinematic distance $D = 12.5 \pm 1.5$ kpc from the Sun, behind the core of a molecular cloud at 9.4 ± 0.2 kpc. At this distance, GRS 1915 + 105, frequently radiating $\sim 3 \times 10^{38}$ erg s⁻¹ in the X-rays, becomes the most luminous X-ray source in the Galaxy. The total hydrogen column density $N(\text{H}) = 4.7 \pm 0.2 \times 10^{22}$ cm⁻² along the line of sight corresponds to a visual absorption $A_V = 26.5 \pm 1$ magnitudes.

The infrared counterpart of GRS 1915+105 exhibits in the 1.2 μm – 2.2 μm band variations of ~ 1 magnitude in a few hours and of ~ 2 magnitudes over longer intervals of time. In the infrared, GRS 1915 + 105 is strikingly similar to SS 433, and unlike any other known stellar source in the Galaxy. The infrared resemblance in absolute magnitude, color, and time variability, between these two sources of relativistic ejections suggests that GRS 1915 + 105, as SS 433, consists of a collapsed object (neutron star or black hole) with a thick accretion disk in a high-mass-luminous binary system.

Key words: Stars: individual: GRS 1915+105 – Stars: variables: other – ISM: clouds – Gamma rays: observations – Infrared: stars – X-rays: stars

the constellation of Aquila, has shown long periods of violent erratic variations with recurrent rises to maximum luminosity (Harmon et al. 1992; Brandt et al. 1993; Castro-Tirado et al. 1994). The fairly hard spectrum with emission up to 220 keV and variable spectral index between -2 and -2.8 observed by BATSE on the Compton Gamma-Ray Observatory (GRO) indicate that GRS 1915 + 105 is a collapsed object, likely a black hole in a binary system (Harmon et al. 1994). The arcmin location by SIGMA on GRANAT (Finoguenov et al. 1994) allowed the detection of variable radio and infrared counterparts (Mirabel et al. 1994). Follow-up observations with the VLA at centimeter wavelengths led to the discovery of relativistic ejections of plasma clouds with apparent superluminal motions (Mirabel & Rodríguez 1994, 1995; Rodríguez & Mirabel 1995).

Here we report the results from a multi-wavelength approach to determine the distance and environment of this unique X-ray source. The millimeter and centimeter wavelengths observations yield constraints on its kinematic distance and give clues on the environment of the source. This source is located near the galactic plane at $l = 45.4^\circ$, $b = -0.3^\circ$ and due to interstellar extinction it is better observed in the infrared (Mirabel et al. 1994). To constrain the nature of the binary system, imaging and spectroscopic observations were carried out in the J (1.25 μm), H (1.65 μm), and K (2.2 μm) bands. The comparison between this source and other well known X-ray binaries is also discussed.

1. Introduction

Since its discovery on 15 August 1992 by the WATCH all-sky X-ray monitor on board of GRANAT (Castro-Tirado et al. 1992), the hard X-ray transient GRS 1915 + 105 in

2. Interstellar gas in the direction to GRS 1915 + 105

2.1. Observations of the atomic hydrogen

Using the Very Large Array (VLA) in configuration D on 16 December 1993, Rodríguez et al. (1995) observed with

Send *off-*print requests to: S. Chaty (chaty@discovery.saclay.cea.fr) or I.F. Mirabel (mirabel@discovery.saclay.cea.fr)

a resolution of 10.3 km s^{-1} the $\lambda 21 \text{ cm}$ line absorption spectra of H I along the lines of sight to GRS 1915 + 105 and to the H II region G 45.46 + 0.06. The latter is the closest H II region on the sky at a projected distance of 17 arcmin from the high-energy source. Its radial velocity with respect to the local standard of rest (LSR) is $+53.6 \pm 1 \text{ km s}^{-1}$. The kinematic distance of this H II region can be unambiguously known combining the $\lambda 21 \text{ cm}$ absorption with the H109 α and H110 α emission (Downes et al. 1980; Matthews et al. 1977; Baud 1977). Assuming that the Sun is at a Galactocentric distance of 8.5 kpc, the H II region is at $\sim 8.8 \text{ kpc}$ from the Sun. The $\lambda 21 \text{ cm}$ opacities toward GRS 1915 + 105 are shown in Fig. 1. Since there is absorption in both the H II region and GRS 1915 + 105 up to 70 km s^{-1} (which corresponds to the LSR velocity of the subcentral point for the galactic longitude $45^\circ 4$), both the H II region and GRS 1915 + 105 are beyond 6 kpc from the Sun (Radhakrishnan et al. 1972).

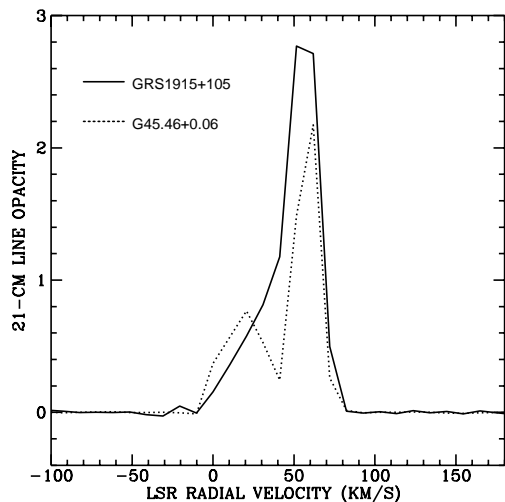


Fig. 1. Opacities of $\lambda 21 \text{ cm}$ line from atomic hydrogen absorption spectra observed along the lines of sight to GRS 1915+105 and to the H II region G 45.46 + 0.06 (Rodríguez et al. 1995) with the VLA in configuration D on 16 December 1993. The resolution is 10.3 km.s^{-1} . Note that the line of sight to GRS 1915 + 105 exhibits a relative excess of H I absorption at LSR radial velocity $41 \pm 6 \text{ km s}^{-1}$.

The line of sight to GRS 1915+105 exhibits additional H I absorption at $41 \pm 6 \text{ km s}^{-1}$ relative to the line of sight to G 45.46 + 0.06, implying that this additional H I absorption is farther than the H II region G 45.46 + 0.06. So GRS 1915 + 105 appears to be behind an H I cloud,

which is at a kinematic distance of $9.4 \pm 0.5 \text{ kpc}$, beyond G 45.46 + 0.06. On the other hand, since there is no absorption at negative velocities below -25 km s^{-1} , GRS 1915+105 must be at a kinematic distance $\leq 14 \text{ kpc}$, which is consistent with the relativistic upper limit of the distance derived by Mirabel & Rodríguez (1994). Therefore we can constrain the kinematic distance of GRS 1915 + 105 to the range $7.9 \leq D \text{ (kpc)} \leq 14$. The H I absorption denotes a column density of atomic gas $N(\text{H I}) = (1.73 \times 10^{22})(T_s/100 \text{ K}) \text{ cm}^{-2}$, where T_s is the spin temperature. This column density is 1.42 times the column density along the line of sight to the H II region G 45.46 + 0.06. Assuming a constant H I absorption per unit length, GRS 1915 + 105 would then be at a kinematic distance $D = 12.5 \pm 1.5 \text{ kpc}$ (Rodríguez et al. 1995).

2.2. Observations of the molecular gas

Low resolution observations of the interstellar molecular gas have been discussed by Castro-Tirado et al. (1994) and Grindlay (1994). Using the Columbia CO survey (Dame et al. 1986), they found that along the line of sight to GRS 1915 + 105 there are molecular gas complexes at the kinematic distances of 1.5 and 7.8 kpc. However, due to the low angular resolution of the Columbia survey, no molecular cloud core was detected on the line of sight, and therefore no evidence for association between the source and a giant molecular cloud was found.

We used the 30 m radiotelescope of the Institut de Radioastronomie Millimétrique (IRAM) for a search in the direction of GRS 1915 + 105 of molecular gas associated with the additional H I absorption detected with the VLA at $41 \pm 6 \text{ km s}^{-1}$. The observations were made from 12 to 19 October 1994, with the 3 mm-receiver, at the rest frequency 115.271204 GHz of the ^{12}CO ($J = 1 - 0$) transition. This transition is a good density tracer, for molecular hydrogen densities of $100 - 300 \text{ cm}^{-3}$ (Sanders et al. 1983). We chopped against an off region, which was conveniently chosen, so that it contains no feature. The coordinates of this reference off region are: $\alpha(1950) = 19^{\text{h}}06^{\text{m}}38^{\text{s}}.2$, $\delta(1950) = 11^{\circ}03'39''$.

Figure 2 shows the ^{12}CO ($J = 1 - 0$) spectrum toward GRS 1915 + 105. There is an emission peak of the CO at the velocity $41.5 \pm 1 \text{ km s}^{-1}$, close to the LSR velocity of the atomic component that causes the additional absorption in H I. In the following we assume that the H I absorption detected with the VLA at the velocity $41 \pm 6 \text{ km s}^{-1}$ and the CO feature detected with the 30 m telescope of the IRAM at $41.5 \pm 1 \text{ km s}^{-1}$ come from the same cloud. Therefore we adopt the far distance for the CO component, and its Doppler shift corresponds to a kinematic distance of $9.4 \pm 0.2 \text{ kpc}$. The velocity width of the molecular cloud is $1.9 \pm 0.1 \text{ km s}^{-1}$.

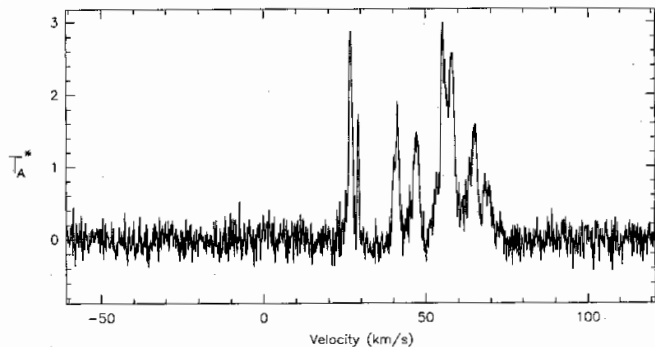


Fig. 2. ^{12}CO ($J = 1 - 0$) emission in the direction of GRS 1915 + 105 observed with the IRAM 30 m telescope.

To study the distribution of the molecular gas at given Doppler shifts, we made maps of the CO emission with velocities covering the following intervals in km.s^{-1} : $(-10, 0)$, $(0, 10)$, $(23, 30)$, $(26, 28)$, $(28, 30)$, $(40, 43)$, $(43, 46)$, $(46, 50)$, $(57, 60)$, $(60, 62)$, and $(62, 70)$. With these intervals of velocities we mapped the CO emission with kinematic distances as far as 12.8 kpc. The only map that shows a local maximum of the CO emission near the projected position of GRS 1915 + 105 is the map of the CO detected in the range of velocities between 40 and 43 km s^{-1} , centered at 41.5 km s^{-1} . This map is shown in Fig. 3. From it we can conclude that GRS 1915 + 105 is behind the core of a molecular cloud located at the kinematic distance $D = 9.4 \pm 0.2$ kpc from the Sun.

The molecular cloud superimposed upon the position of GRS 1915 + 105 has a diameter of 1.05 arcmin, which corresponds to a physical size of 2.9 pc for a kinematic distance of 9.4 kpc. Thus, the mean density of the molecular cloud is $\sim 400 \text{ cm}^{-3}$. One can derive the mass of the cloud using the equation $M(\text{H}_2) = 1.3 \times 10^3 S D^2$, where $S = 1.24 \times 10^{-2} \text{ K km s}^{-1} \text{ deg}^2$ is the apparent CO luminosity of the cloud (Dame et al. 1986). The cloud mass is $M(\text{H}_2) = 1400 \pm 100 M_\odot$. The column density of molecular hydrogen H_2 is $N(\text{H}_2) = 3.6 \times 10^{20} \int T_A^*(\text{CO}) dv = 1.5 \pm 0.1 \times 10^{22} \text{ cm}^{-2}$, where the integrated antenna temperature is $T_A^*(\text{CO}) = 31.027 \text{ K}$, and the averaged velocity width is $dv = 1.3 \text{ km s}^{-1}$. So the total hydrogen column density is $N(\text{H}) = N(\text{H1}) + 2N(\text{H}_2) = 4.7 \pm 0.2 \times 10^{22} \text{ cm}^{-2}$. This is consistent, within the errors, with the column density of $\sim 5 \times 10^{22} \text{ cm}^{-2}$ derived from the ROSAT X-ray spectrum of the source (Greiner et al. 1994). The visual absorption derived from the column density, using the equation $A_v(\text{mag}) = 5.59 \times 10^{-22} N(\text{H})(\text{cm}^{-2})$ (Predehl & Schmitt 1995), is $A_v = 26.5 \pm 1$ magnitudes.

3. The infrared counterpart of GRS 1915 + 105

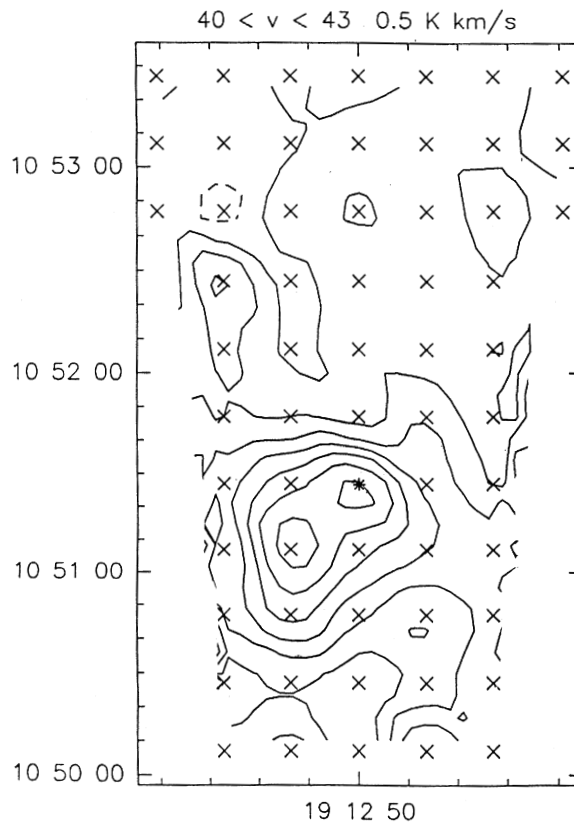


Fig. 3. Map of the ^{12}CO ($J = 1 - 0$) emission for the LSR velocity $40 \leq v \leq 43 \text{ km s}^{-1}$ in the direction of GRS 1915 + 105. The asterisk indicates the position of the VLA radio counterpart of the high-energy source. The contours are -0.5, 0.5 to 3.5 by 0.5, in units of $\text{K T}_A^* \text{ km s}^{-1}$ for a LSR velocity interval of 40 to 43 km.s^{-1} . The observed positions are represented by crosses. Coordinates are in the B1950 equinox.

3.1. Infrared observations

Mirabel et al. (1994) had shown that there is no visual counterpart of GRS 1915 + 105 brighter than $R = 21$ magnitudes. Using the NTT with a Gunn-z filter on 9 July 1994, we observed at $\sim 1 \mu\text{m}$ a faint counterpart consistent with the $I = 23.4$ magnitudes counterpart reported by Boër et al. (1995).

We carried out infrared observations of GRS 1915+105 at the European Southern Observatory (ESO) with the ESO/MPI 2.2 m telescope on 4 and 5 June 1993 with the IRAC2 camera (Mirabel et al. 1994), and from 5 to 8

July 1994 with the IRAC2b camera in the J ($1.25 \mu\text{m}$), H ($1.65 \mu\text{m}$) and K ($2.2 \mu\text{m}$) bands. The IRAC2(b) camera was mounted at the F/35 infrared adapter of the telescope. This camera is a Rockwell 256×256 pixels Hg: Cd:Te NICMOS 3 large format infrared array detector. It was used with the lens C, providing an image scale of $0.49 \text{ arcsec/pixel}$ and a field of $136 \times 136 \text{ arcsec}^2$. The typical seeing for these observations was 1.2 arcsec .

Follow-up observations were performed on our request by S. Massey at the 3.6 m Canada-France-Hawaii Telescope (hereafter CFHT) on Mauna Kea on 16 August 1994, with the Redeye camera, in the H and K bands. The narrow field infrared Redeye camera was mounted at the F/8 focus of the CFHT. This camera is a Rockwell 256×256 pixels Hg: Cd:Te NICMOS 3 infrared array detector, providing a plate scale of $0.20 \text{ arcsec/pixel}$. The typical seeing for these observations was 0.6 arcsec .

Each image taken at la Silla is the median of 5 images exposed during 2 minutes. After taking each image of the object, an image of the sky was taken, to allow subtraction of the blank sky. For the images acquired by the CFHT, the result is the median of 18 images exposed during 30 s. The images are further treated by removal of the bias, the dark current, and the flat field, and we carried out absolute and relative photometry, to look for small variations of the luminosity of GRS 1915 + 105. This work was performed with the IRAF procedures, using the DAOPHOT package for the photometry in crowded fields.

The magnitudes are given in Table 1, and the variations in the K-band are shown in Fig. 4. We can see that GRS 1915 + 105 exhibits strong variability in the J, H and K bands. The luminosity of GRS 1915 + 105 increased by nearly 1 magnitude in H and K between the nights of 4 and 5 June 1993. Between 4 June 1993 and 5 July 1994 there was a change by nearly 2 magnitudes in J, 2.5 magnitudes in H, and 2.1 magnitudes in K. However, no variations greater than 0.1 magnitudes were detected in the period 5–8 July 1994 (we took 1 image each 30 minutes during 5 hours, on 5 and 6 July 1994). From Table 1 it seems that the infrared colors change with luminosity.

Figure 4 shows that GRS 1915 + 105 exhibits short-term variability in intervals of less than 24 hours as well as long-term variability over intervals from one month to one year. The rapid increase of 1 magnitude observed in an interval of 24 hours in June 1993 could result from occultation. It is also interesting to note that this rapid variation of the infrared luminosity occurred in a period when the source was strong and showing rapid variations of luminosity in the 8–60 keV energy band observed by WATCH (Sazonov et al. 1994), and in the 20–100 keV energy band observed by BATSE (Harmon et al. 1994; Paciesas et al. 1995). The luminous infrared phase of GRS 1915 + 105

observed in July 1994 corresponds to a period of erratic variations in the X-rays, when the source was fainter in the 20–100 keV energy band than in the period June 1993 (Harmon et al. 1994; Paciesas et al. 1995).

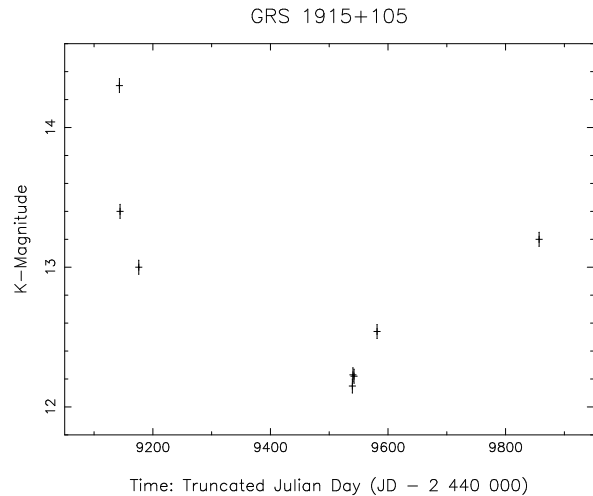


Fig. 4. Time variation of K-band ($2.2 \mu\text{m}$) luminosity of the source GRS 1915 + 105 from 4 June 1993 until 19 May 1995.

3.2. Discussion

From the apparent magnitudes in Table 1 we derived the absolute magnitudes, corrected for interstellar extinction, using a visual absorption of $A_v = 26.5 \pm 1$ magnitudes, and the kinematic distance $D = 12.5 \pm 1.5 \text{ kpc}$. The absorptions in the J, H, and K bands are respectively $A_J = 7.1 \pm 0.2$, $A_H = 4.1 \pm 0.2$, and $A_K = 3.0 \pm 0.1$ magnitudes. The infrared absolute magnitudes and colors of GRS 1915 + 105 and other well known X-ray galactic sources during minimum and maximum luminosity are listed in Table 2. To derive the absolute magnitudes of SS 433 we assumed the kinematic distance of $4.2 \pm 0.5 \text{ kpc}$ (van Gorkom et al. 1982) and a visual absorption $A_v = 7.25 \pm 0.25$ magnitudes (McAlary & McLaren 1980). In view that the distance to SS 433 is somewhat uncertain, in the following we use its kinematic distance derived from HI absorption, namely, using the same method used to derive the distance to GRS 1915 + 105 (Mirabel & Rodríguez 1994). The estimated errors of the absolute magnitudes in Table 2 take into account the uncertainties on the distance and interstellar absorption.

The infrared emission of GRS 1915 + 105 cannot arise **only** in the photosphere of the secondary star: 1) be-

Table 1. Optical and infrared magnitudes of GRS 1915+105.

Date	TJD ¹	telescope	R(0.7 μm)	I(0.9 μm)	J(1.25 μm)	H(1.65 μm)	K(2.2 μm)
19/04/93	9097	Pic Midi	> 21	-	-	-	-
04/06/93	9143	ESO 2.2m	-	-	$\geq 18 \pm 0.2$	16.2 ± 0.2	14.3 ± 0.2
05/06/93	9144	ESO 2.2m	-	-	18 ± 0.1	15.0 ± 0.1	13.4 ± 0.1
27/06/93 ²	9166	CFHT	> 26.1	23.4 ± 0.3	-	-	-
07/07/93 ³	9176	UKIRT	-	-	16.6 ± 0.1	-	13.0 ± 0.1
05/07/94	9539	ESO 2.2m	-	-	16.2 ± 0.1	13.7 ± 0.1	12.15 ± 0.08
06/07/94	9540	ESO 2.2m	-	-	-	-	12.23 ± 0.04
07/07/94	9541	ESO 2.2m	-	-	-	-	12.23 ± 0.1
08/07/94	9542	ESO 2.2m	-	-	-	-	12.22 ± 0.1
09/07/94	9543	NTT	> 22	-	-	-	-
16/08/94	9581	CFHT	-	-	-	14.83 ± 0.1	12.54 ± 0.1
19/05/95 ⁴	9857	UKIRT	-	-	-	-	13.2 ± 0.1

¹Truncated Julian Date (JD - 2 440 000).

²From Boër et al. (1995).

³From Castro-Tirado et al. (1993).

⁴From Geballe (1995).

Table 2. J, H, and K absolute magnitudes of X-ray sources.

Source	J(1.25 μm)	H(1.65 μm)	K(2.2 μm)	J-K	H-K	J-H	ref
GRS 1915 + 105	-4.5 ± 0.9	-4.6 ± 0.9	-5.1 ± 0.8	0.6	0.5	0.1	1
	-6.3 ± 0.9	-5.8 ± 0.9	-6.4 ± 0.8	0.1	0.6	-0.5	2
SS 433	-5.2 ± 0.8	-5.0 ± 0.7	-5.5 ± 0.7	0.3	0.5	-0.2	3
	-6.4 ± 0.8	-6.4 ± 0.7	-6.8 ± 0.7	0.4	0.4	0.0	
Cyg X-3	-3.3 ± 0.3	-4.1 ± 0.3	-4.9 ± 0.3	1.6	0.8	0.8	4,5,6
	-3.7 ± 0.3	-4.8 ± 0.3	-5.7 ± 0.3	2	0.9	1.1	
Cyg X-1	-5.9 ± 0.2	-5.8 ± 0.2	-5.8 ± 0.2	-0.1	0.0	-0.1	7,8
	-6.4 ± 0.2	-	-6.3 ± 0.2	-0.1	-	-	

¹see Table 1 on 05 June 1993

²see Table 1 on 05 July 1994

³Catchpole et al. 1981

⁴Joyce 1990

⁵Jones et al. 1994

⁶Becklin et al. 1972

⁷Leahy & Ananth 1992

⁸Beall et al. 1984

cause of the shape of the spectrum, which cannot be reproduced by photospheric emission from any stellar type (e.g. Koornneef 1983), and 2) because of the rapid variations in luminosity and energy distribution (see Table 1). Therefore, besides the photospheric emission from the secondary, there must be in GRS 1915 + 105 an additional source of infrared emission.

The energy distribution of the most well studied X-ray galactic sources is shown in Fig. 5. Besides the time variations, the infrared absolute magnitudes and colors of GRS 1915 + 105 are strikingly similar to the classic source

of relativistic jets SS 433 (Margon 1984). This similarity in the observed infrared properties suggests that SS 433 and GRS 1915+105 are systems of similar nature. The infrared emission of SS 433 arises in a high-mass binary of type late O or early B (Clark & Milone 1980; Wynn-Williams & Becklin 1979) or Be (Campbell & Thompson 1977), with possible contributions of free-free emission from an ionized plasma at $T \sim 7500$ K (McAlary & McLaren 1980), an accretion disk (Kodaira et al. 1985), and/or even the jets (Catchpole et al. 1981).

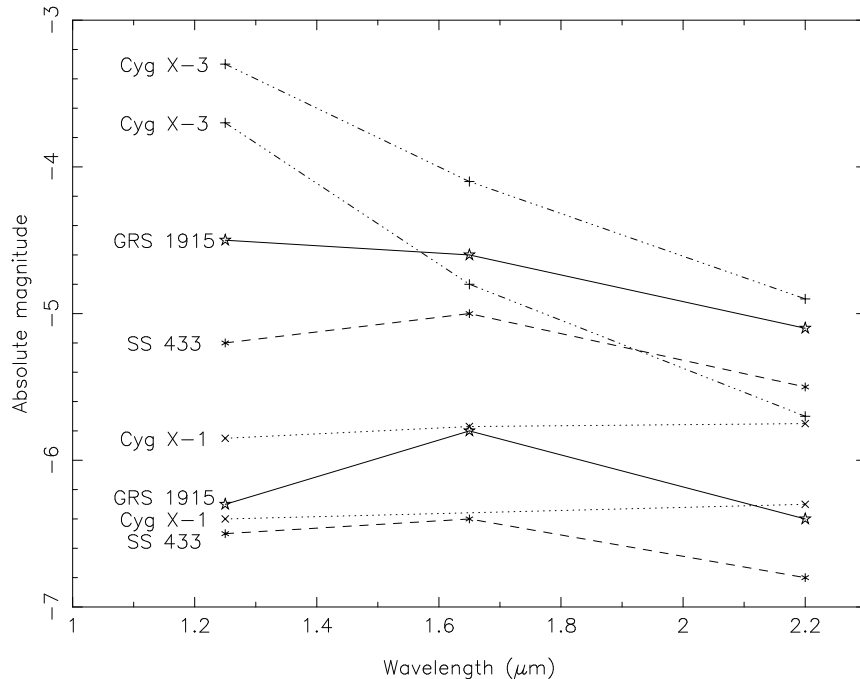


Fig. 5. Infrared energy distributions of GRS 1915 + 105, SS 433, Cyg X-1 and Cyg X-3 for the periods of minimum and maximum luminosity.

Within the context of a binary model with an accretion disk, Kodaira et al. (1985) conclude that the observed infrared flux in the SS 433 system comes mostly from an accretion disk around the compact object of the binary system, and that the day-to-day variations may be due to different configurations of disk structures, depending on the mass supply and the internal magnetohydrodynamic balances. Therefore, by analogy with SS 433 (Margon 1984), GRS 1915 + 105 would be a collapsed object with a thick accretion disk in a hot and luminous high-mass binary.

4. Conclusion

Millimeter and centimeter observations show that GRS 1915 + 105 is at a kinematic distance from the Sun of 12.5 ± 1.5 kpc, behind the core of a molecular cloud at 9.4 ± 0.2 kpc. The column density of molecular gas $N(\text{H}_2) = 1.5 \pm 0.1 \times 10^{22} \text{ cm}^{-2}$, combined with the $\lambda 21$ cm HI absorption, imply a total column density $N(\text{H}) = 4.7 \pm 0.2 \times 10^{22} \text{ cm}^{-2}$, which corresponds to a visual absorption in the line of sight $A_V = 26.5 \pm 1$ magnitudes.

At a distance of 12.5 kpc the hard X-ray transient GRS 1915 + 105 often becomes the most powerful X-ray emitter in the Galaxy. The X-ray light curve observed since its discovery in 1992 (Paciesas et al. 1995) shows that, for recurrent periods that last several months it is one of the brighter sources of the sky at energies ≥ 20 keV. At 12.5 kpc its X-ray luminosity is $\sim 3 \times 10^{38} \text{ erg s}^{-1}$, which is indicative of super-Eddington accretion for a collapsed object of stellar mass.

The infrared counterpart of the source presents short- and long-term variations. We have observed a change of one magnitude over an interval of 24 hours, and changes of two magnitudes over intervals of months. No periodicity was detected. The similarity at infrared wavelengths between GRS 1915 + 105 and SS 433 suggests that both sources of relativistic jets are systems of similar nature. This similarity, together with the time variability of the infrared counterpart of GRS 1915 + 105, indicates that a large fraction of the infrared emission may come from an accretion disk. Following the analogy with SS 433, GRS 1915 + 105 would be a collapsed object (neutron star or black hole) with a thick accretion disk in a high-mass and luminous binary system.

Acknowledgements. We thank S. Massey for the infrared images obtained with the CFHT, T. Geballe and P. Charles (UKIRT Service program) for the K-magnitude of GRS 1915+105 on 19 May 1995. We acknowledge helpful conversations with Christian Motch and Christian Gouiffes. We also thank John Simmons for reading the manuscript, and the anonymous referee for helpful suggestions.

References

- Baud B., 1977, *A&A*, 57, 443
 Beall J.H., Knight F.K., Smith H.A. et al., 1984, *ApJ*, 284, 745
 Becklin E.E., Kristian J., Neugebauer G., Wynn-Williams C.G., 1972, *Nat. Phys. Sci.*, 239, 130
 Boër M., Greiner J., Motch C., 1995, *A&A* in press
 Brandt S., Castro-Tirado A.J., Lund N., 1993, *IAU Circ.* 5779
 Campbell M.F., Thompson R.I., 1977, *NASA TM X-73*, p. 190
 Castro-Tirado A.J., Davies J., Brandt S., Lund N., 1992, *IAU Circ.* 5590
 Castro-Tirado A.J., Davies J., Brandt S., Lund N., 1993, *IAU Circ.* 5830
 Castro-Tirado A.J., Brandt S., Lund N. et al., 1994, *ApJS* 92, 469
 Catchpole R.M., Glass I.S., Carter B.S., Roberts G., 1981, *Nat*, 291, 392
 Clark T.A., Milone E.F., 1980, *PASP*, 93, 338
 Dame T.M., Elmegreen B.G., Cohen R.S., Thaddeus P., 1986, *ApJ*, 305, 892
 Downes D., Wilson T.L., Bieging J., Wink J., 1980, *A&AS*, 40, 379
 Finoguenov F., Churazov E., Gilfanov M. et al., 1994, *ApJ*, 424, 940
 Geballe T., 1995, private communication
 Ghigo F.D., Waltman E.B., Foster R.S., 1995, *IAU Circ.* 6204
 Greiner J., Snowden S., Harmon B.A., Kouveliotou C., Paciasas W., 1994. In: Fichtel C.E., Gehrels N., Norris J.P (eds.) *AIP Conference Proceedings* 304. AIP Press, New York, p. 260
 Grindlay J.E., 1994, *ApJS* 92, 465
 Harmon B.A., Paciasas W.A., Fishman G.J., 1992, *IAU Circ.* 5619
 Harmon B.A., Zhang S.N., Wilson C.A. et al., 1994. In: Fichtel C.E., Gehrels N., Norris J.P (eds.) *AIP Conference Proceedings* No 304. AIP Press, New York, p. 210
 Jones T.J., Gehrz R.D., Kobulnicky H.A., Molnar L.A., Howard E.M., 1994, *AJ*, 108, 605
 Joyce R.R., 1990, *AJ*, 99, 1891
 Kodaira K., Nakada Y., Backman D.E., 1985, *ApJ*, 296, 232
 Koornneef J., 1983, *A&A*, 128, 84
 Leahy D.A., Ananth A.G., 1992, *MNRAS*, 256, 39p
 Margon B., 1984, *ARA&A*, 22, 507
 Matthews H.E., Goss W.M., Winnberg A., Habing H.J., 1977, *A&A*, 61, 261
 Mc Alary C.W., Mc Laren R.A., 1980, *ApJ*, 240, 853
 Mirabel I.F., Rodríguez L.F., 1994, *Nat*, 371, 46
 Mirabel I.F., Rodríguez L.F., 1995, Review at the 17th Texas Symposium on Relativistic Astrophysics. *Annals of the New-York Academy of Sciences*, eds Boehringer H., in press
 Mirabel I.F., Duc P.-A., Rodríguez L.F. et al., 1994, *A&A*, 282, L17
 Paciasas W.S., Deal K.J., Harmon B.A. et al., 1995, Poster at Third Compton Symposium, Munich
 Predehl P., Schmitt J.H.M.M., 1995, *A&A*, 293, 889
 Radhakrishnan V., Goss W.M., Murray J.D., Brooks J.W., 1972, *ApJS*, 24, 49
 Rodríguez L.F., Mirabel I.F., 1995, *Proceedings of the National Academy of Sciences*, ed. Zensus A., in press
 Rodríguez L.F., Gerard E., Mirabel I.F., Gómez Y., Velázquez A., 1995, *ApJS* in press
 Sanders D.B., Solomon P.M., Scoville N.Z., 1983, *ApJ*, 276, 182
 Sazonov S.Yu., Sunyaev R.A., Lapshov I.Yu. et al., 1994, *Astronomy Letters*, 20, 787
 Sazonov S., Sunyaev R. et al., 1995, *IAU Circ* 6209
 van Gorkom J.H., Goss W.M., Seaquist E.R., Gilmore W.S., 1982, *MNRAS*, 198, 757
 Wynn-Williams C.G., Becklin E.E., 1979, *Nat*, 282, 810